Earth and Planetary Science Letters 430 (2015) 75–85

Contents lists available at ScienceDirect

Earth and Planetary Science Letters

www.elsevier.com/locate/epsl

Mass transfer in the oceanic lithosphere: Serpentinization is not isochemical

Benjamin Malvoisin [a,b,*]

[a] Institute of Earth Sciences, University of Lausanne, Géopolis, 1015 Lausanne, Switzerland
[b] CHYN, University of Neuchâtel, rue Emile Argand 11, 2000 Neuchâtel, Switzerland

ARTICLE INFO

Article history:
Received 11 February 2015
Received in revised form 13 July 2015
Accepted 20 July 2015
Available online xxxx
Editor: J. Brodholt

Keywords:
serpentinization
abyssal peridotites
Si-metasomatism
brucite
volume change
hydrogen

ABSTRACT

Whereas the serpentinization reaction leads to stark differences in the physical properties of mantle rocks at mid-ocean ridges, the chemical changes associated with this reaction are thought to be restricted to the addition of water and the generation of hydrogen ("isochemical" reaction). Here, I compile a geochemical dataset of serpentinized peridotites at mid-ocean ridges evidencing that a decrease by up to 11% of the MgO/SiO_2 ratio is associated with serpentinization. This MgO/SiO_2 decrease is consistent with the calculated distribution of Mg in the minerals since, during isochemical serpentinization, ~10% of the Mg should be contained in brucite, an Mg-hydroxide not commonly observed in serpentinized peridotites, which are typically composed of serpentine ($Mg_3Si_2O_5(OH)_4$) and magnetite (Fe_3O_4). This latter mineralogical assemblage and a decrease of the MgO/SiO_2 ratio were only reproduced in numerical models of peridotite reacting with fluids containing aqueous silica at fluid to rock (F/R) ratios greater than 20. At higher F/R ratios, talc ($Mg_3Si_4O_{10}(OH)_2$) was found to be stable, in agreement with observations in extremely altered samples found at mid-ocean ridges. The potential sources for aqueous silica in the fluid are the alteration of mafic units intruding mantle rocks at slow-spreading ridges. The mineralogical and chemical changes associated with SiO_2 gain during serpentinization at mid-ocean ridges will have consequences on abiotic hydrogen production, contribute to a volume increase of 50% and decrease water incorporation during serpentinization by more than 10% compared to "isochemical" serpentinization. These changes will also increase the depth at which fluids are released by dehydration reactions in subduction zones by more than 20 km.

1. Introduction

Slow-spreading ridges exhume large tracts of mantle-derived ultramafic rocks (Cannat, 1993) and receive a moderate magma supply. Magmatic heat is released through the convection of aqueous fluids in the oceanic crust. When these fluids reach ultramafic rocks, alteration minerals such as serpentine ($Mg_3Si_2O_5(OH)_4$), brucite ($Mg(OH)_2$), talc ($Mg_3Si_4O_{10}(OH)_2$) and magnetite (Fe_3O_4) are formed, and show stark differences in physical and chemical properties compared to the primary minerals. The effect of serpentinization on these properties is already perceptible before the reaction progress even exceeds 10%, with an increase in the recorded magnetization by two orders of magnitude through the production of ferromagnetic magnetite (e.g. Malvoisin et al., 2012a), the formation of a reducing environment through the production of hydrogen (Charlou et al., 2002) and the decrease of the rock strength due to the precipitation of serpentine (Escartín et al., 2001). As the reaction progresses further, serpentinization impacts other properties such as rock density since the newly formed hydrated phases have lower densities ($\rho_{serpentine} = 2900$ kg/m^3) compared to the primary minerals ($\rho_{olivine} = 3300$ kg/m^3). This density change contributes to lower mantle seismic velocities (Miller and Christensen, 1997) and is associated with a positive increase in the solid volume by up to 50% in the case of a reaction where water is the only component to be exchanged (Coleman and Keith, 1971). This volume change has two opposite effects on the permeability which both increases through the generation of fluid pressures high enough to fracture the rock (e.g. Plümper et al., 2012) and decreases when the porosity is filled with secondary phases (Godard et al., 2013). Constraining the chemical and mineralogical changes during serpentinization is thus crucial for understanding reaction-induced evolution of the properties of the oceanic lithosphere.

Fulfilling this latter objective is not straightforward because serpentinization occurs in an open system where the conditions of alteration evolve through time (Andreani et al., 2007). Although the

* Correspondence to: Institute of Earth Sciences, University of Lausanne, Géopolis, 1015 Lausanne, Switzerland. Tel.: +41 0 32 718 26 72.
E-mail address: benjamin.malvoisin@unine.ch.

http://dx.doi.org/10.1016/j.epsl.2015.07.043
0012-821X/

effect of temperature on the distribution of iron between brucite, magnetite and serpentine during serpentinization has been quantified with increasing precision (Malvoisin et al., 2012b; Klein et al., 2013), the influence of reacting system composition on the mineralogical evolution during the reaction is still not constrained. In spite of the extensive geochemical datasets available for peridotites (Niu, 2004; Bodinier and Godard, 2003) and fluid compositions (Charlou et al., 2002) at mid-ocean ridges, the respective roles of the initial composition of the system and the mass transfer during the reaction on the final composition have yet to be determined. Mass transfer during serpentinization mainly involves the addition of water and fluid-mobile elements (e.g. B, Li, Cl, As, Sb, U, Th, Sr) susceptible to be released when entering subduction zones (see Deschamps et al., 2013 for a review). Based on the measurement of constant oxides/SiO_2 ratios with the increase in reaction progress (Coleman and Keith, 1971; Komor et al., 1985), the transfer of major elements during serpentinization is thought to be negligible in the general case and the reaction is thus called "isochemical" (Mével, 2003; Deschamps et al., 2013). However, some studies reported changes in the bulk composition of mantle-derived rocks at mid-ocean ridges. Snow and Dick (1995) and Niu (2004) measured a decrease of the MgO/SiO_2 ratio but they attributed this change in composition not to serpentinization itself but instead to low-temperature alteration on the seafloor. Some instances of large changes in the MgO/SiO_2 ratio of abyssal peridotites have been reported during talc formation. At the Atlantis Massif, these changes were interpreted as resulting from the serpentinization reaction itself with a synchronous formation of talc and serpentine (Boschi et al., 2008). At the 15°20′ fracture zone, they were attributed to a high temperature event with Si-rich fluids forming talc at the expense of serpentine (Paulick et al., 2006; Harvey et al., 2014).

Here I use a statistical approach to determine the respective role on abyssal peridotite composition of both the system's initial composition and the change in composition due to fluid/rock interactions at mid-ocean ridges. Further, I thermodynamically model fluid/mantle rock interactions to determine the mineralogical and chemical processes controlling compositional changes and their impact on the physical and chemical properties of the mantle rocks exhumed at mid-ocean ridges.

2. Methodology

2.1. Determining changes in composition during serpentinization with geochemical data compilation

I assembled a dataset consisting of bulk rock major element analyses of 1075 serpentinized harzburgites, dunites and lherzolites, 551 of which were abyssal peridotites compiled from 18 sources and 524 of which were ophiolitic peridotites compiled from 34 sources (see Supplementary Table S1 for details and Bodinier and Godard (2003) for a referencing of the ophiolites).

I targeted the variations in MgO and SiO_2, the two most abundant components in abyssal peridotites, in order to estimate their deviation in composition from the "isochemical" model. These variations depend on the protolith composition and mass transfer during processes such as serpentinization. The influence of the protolith composition was modeled differently depending on its nature. Unaltered dunites are mainly composed of olivine with a constant MgO/SiO_2 ratio of 1.2 (Niu et al., 1997) which was considered representative of the protolith composition. More complex changes in protolith composition from fertile lherzolites to refractory harzburgites were modeled by a progressive magmatic depletion of a primitive mantle following Jagoutz et al. (1979) and Hart and Zindler (1986). This model predicts that the protoliths of serpentinized lherzolites and harzburgites should lie on a straight line, the so-called "terrestrial array", in MgO/SiO_2 vs. Al_2O_3/SiO_2 diagrams. As this array was determined with analyses of fresh continental peridotites, it must be tested against data of unaltered peridotites formed at mid-ocean ridges to be used here. From a geochemical perspective, serpentinization is a process during which water is incorporated into mineral phases. To estimate the weight fraction of this bound water in the rock, the loss on ignition (LOI) is measured by heating a powdered sample in a furnace to temperatures of ∼1000 °C. Samples with low LOI and thus with low degrees of serpentinization were selected in the database for determining the deviation of unaltered abyssal peridotites from the "terrestrial array". Other volatile components such as CO_2 can participate in an increase of the LOI (e.g. Schwarzenbach et al., 2013). Carbonate-bearing samples were therefore not included in the compilation. Abyssal peridotites are generally extensively altered as shown by the fact that only 3% of the selected samples have LOI below 4 wt.%. As this is not enough for accurately estimating the deviation from the terrestrial array, ophiolites samples were considered, since 25% of these samples have LOI $<$ 4 wt.%. Moreover, irrespective of the mechanism of serpentinization of the two types of serpentinized peridotites, at decreasing levels of hydration these samples should project back to a common origin.

2.2. Thermodynamic modeling

Fluid/rock interactions were modeled at the scale of geochemical data acquisition, i.e. at the bulk rock scale rather than at the grain scale. Serpentinization relies on two kinds of mineralogical reactions: dissolution reactions releasing aqueous species in the fluid and precipitation reactions allowing the incorporation of new mineral species in the rock. The nature and the extent of these reactions depend both on their kinetics and on thermodynamic equilibrium. Malvoisin et al. (2012b) demonstrate experimentally using powders that the kinetics of serpentinization are controlled by the dissolution of olivine rather than by the precipitation of secondary phases. Therefore, the bulk composition of the reacting part of the rock was assumed here to depend on the kinetics of dissolution of the primary minerals. The mineralogical composition of the reacted peridotite was then determined with thermodynamic modeling tools by neglecting the kinetics of precipitation and by assuming a constant temperature and an initial composition of the reacting system only dependent on the reaction progress and on the initial composition of the peridotite (no spatial variability). These assumptions are shown to be valid in the Supplementary materials P1.

Seismic velocity profiles indicate that serpentinization mainly occurs within the first three kilometers of the oceanic lithosphere (Canales et al., 2000). In these domains, lithostatic pressure variations do not exceed 100 MPa whereas temperature can vary by more than 400 °C. Therefore, the variations of thermodynamic properties due to pressure variations are negligible compared to those associated with temperature variations. All numerical simulations were thus conducted at a constant pressure of 50 MPa. The four parameters considered here as having a potential impact on the composition of serpentinized peridotites at mid-ocean ridges are: temperature, bulk composition of the reacting protolith, composition of the fluid, and relative quantity of protolith and fluid during the alteration (fluid to rock ratio). Two different numerical models were used to understand compositional change during serpentinization.

2.2.1. "Isochemical" serpentinization model

A first model was built to determine the influence of the starting composition of the reacting protolith on the nature and the composition of the secondary minerals during "isochemical" serpentinization. This model was aimed at providing a basis for com-

parison with mineralogical observations in natural rocks. To reproduce "isochemical" serpentinization, exchanges in oxygen and hydrogen between the solid and the fluid phases were the only exchanges allowed and hydration and redox reactions were thus the only modeled processes. The thermodynamic model of Malvoisin et al. (2012a) was used with the database of Klein et al. (2009). This model considers the incorporation of iron as ferrous iron in brucite and as both ferrous and ferric iron in serpentine. The composition of the reacting solid depends both on the modes of the minerals in the unreacted protolith and on the reaction progress. Indeed, at temperatures below ~350 °C where olivine is unstable (Klein et al., 2013), the reaction rate of olivine (r_{ol}) is 14 times higher than that of pyroxene (r_{opx}; Bach et al., 2004; Ogasawara et al., 2013). Therefore, values of $r_v = r_{ol}/r_{opx} > 1$ were used. A parameter was defined for investigating the influence of the unreacted protolith composition: $X_{ol} = n_{oli}/(n_{oli} + n_{opxi})$ with n_{oli} and n_{opxi} the initial amounts of olivine and orthopyroxene, respectively. Olivine and orthopyroxene compositions were fixed to $(Mg_{0.9}Fe_{0.1})_2SiO_4$ and $(Mg_{0.9}Fe_{0.1})SiO_3$, respectively, in agreement with their respective average Mg/(Mg + Fe) ratios in abyssal peridotites of 0.9029± 0.0037 and 0.9068 ± 0.0055 (Niu et al., 1997). Because these standard deviations are smaller than 1%, the variability of these compositions was not accounted for in the model. This model also ignores Ca-bearing phases such as clinopyroxenes, which can represent several percents of the unreacted mineralogy in abyssal peridotites (Niu, 2004). Nevertheless, this simplification is not expected to strongly impact the results since clinopyroxene remains stable in a wide range of conditions at temperatures below 350 °C (Klein et al., 2013). For each X_{ol} of the considered range, the reaction progress was progressively increased and defined as: $\xi = \frac{n_r}{n_i}$ with n_r the amount of reacted olivine and orthopyroxene and $n_i = n_{oli} + n_{opxi}$. As $r_v > 1$, n_r is not directly proportional to n_i but can be expressed as: $n_r = r_{ol} * n_{oli} + r_{opx} * n_{opxi}$ if olivine remains in the system, or as $n_r = n_{oli} + r_{opx} * n_{opxi} * t$ if olivine has been consumed completely. t denotes the duration of the reaction.

2.2.2. Modeling fluid/rock interactions during serpentinization

The second model is an "open-system" model that aims at investigating the influence of temperature, fluid composition and mass of fluid over mass of reacting protolith (F/R ratio) on mass transfer between the fluid and the solid. In this model, the protolith composition is fixed and divided in a reacting part and a non-reacting part. As shown above, the composition and proportion of each part depend on the composition of the reacting peridotite and on the reaction progress. Here, a molar mean reaction progress of 80 ± 20% was determined using the volumetric mean calculated by Cannat et al. (2010) from the observation of thin-sections prepared on rocks drilled in the first 200 m of the crust in the MAR 23°N region. As the mineralogical and geochemical data compiled here were acquired on samples recovered with the same sampling methods (i.e. by drilling or dredging), this estimate of reaction progress should be representative of the natural samples used here for comparison. A mean unreacted peridotite composition of 59.9 ± 9.2, 37.1 ± 9.0 and 3.0 ± 2.3 mol.% of olivine, orthopyroxene and clinopyroxene, respectively, was calculated by using 73 estimates of the mineral proportions in unaltered peridotites (Niu, 2004). These estimates rely on corrections for alteration and are thus associated with significant errors. However, they represent the largest available dataset for unaltered abyssal peridotites modal composition to date. Moreover, calculations performed with ± 5 mol.% of olivine in the unreacted peridotite show that the variations of the MgO/SiO_2 investigated here only slightly depend on the initial composition of the unaltered peridotite. The unreacted peridotite composition gives an olivine modal proportion of 65.9 ± 10.1 vol.% with a maximum in agreement with the data of Bodinier and Godard (2003). Using the values of the average reaction progress and of r_v (Cannat et al., 2010; Ogasawara et al., 2013), the following composition was obtained for the protolith: 59.9, 18.6 and 1.5 mol.% of olivine, orthopyroxene and clinopyroxene, respectively, for the reacting part and 18.4 and 1.5 mol.% of orthopyroxene and clinopyroxene, respectively, for the non-reacting part. The same compositions as for the "isochemical model" were used for olivine and orthopyroxene, and initial clinopyroxene composition was fixed to $Ca(Mg_{0.9}Fe_{0.1})Si_2O_6$. Three types of fluids found at slow-spreading ridges were used: seawater and two hydrothermal fluids expelled at vents located on mafic basements (mafic-related vent fluids, MRV) or on ultramafic basements (ultramafic-related vent fluids, URV fluids). Their composition was determined with the data of Charlou et al. (2002) reporting 5 MRV and 2 URV fluids compositions from hydrothermal fields located on the Mid-Atlantic ridge. The compositions of MRV and URV fluids mainly differ in their amount of dissolved silica which is 3 times higher in MRV than in URV fluids and of dissolved hydrogen which is 30 times higher in URV than in MRV (Table 1). Vent fluids do not contain Mg whereas seawater contains 50 mM of Mg. These compositions are in agreement with the thermodynamic calculations of Wetzel and Shock (2000) predicting the composition of fluids in equilibrium with mafic or ultramafic rocks. The F/R ratio ranged from 0.2 to 10^5 with the lowest value set by the B-dot equation used to calculate the ionic strength (Klein et al., 2009). A Matlab® code was written to automatically generate inputs with different F/R ratios for the EQ3/6 software (Wolery, 1992). For each F/R ratio, the influence of temperature on the composition of the rock was then investigated by using the procedure described in Klein et al. (2013). The thermodynamic database of Klein et al. (2013) was used with solid solutions for olivine ($(Mg,Fe)_2SiO_4$), orthopyroxene ($(Mg,Fe)SiO_3$), clinopyroxene ($Ca(Mg,Fe)Si_2O_6$), serpentine (with the following end-members: chrysotile, greenalite (ferrous serpentine), kaolinite and cronstedtite (ferric and ferrous serpentine)), brucite ($(Mg,Fe)(OH)_2$), talc ($(Mg,Fe)_3Si_4O_{10}(OH)_2$), chlorite ($(Fe,Mg)_5Al_2Si_3O_{10}(OH)_8$) and tremolite ($Ca_2(Mg,Fe)_5Si_8O_{22}(OH)_2$). The reductions of sulfate and carbon by $H_{2,aq}$ were suppressed.

Table 1
Composition of the fluid used in modeling. Fluid compositions used in the "open" model (values are in mM).

	Seawater	Mafic fluid	Ultramafic fluid
pH	7.8	3.5	3
$SiO_{2,aq}$	0.1	20	7
Cl	546	500	600
Na	464	450	500
K	9.8	20	20
Mg	53	0	0
Ca	10.2	20	30
Fe	1.50E−06	2	5
HCO_3^-	2.3	10	10
$O_{2,aq}$	0.25	–	–
$H_{2,aq}$	–	0.3	10

The compositions were calculated by averaging the data of Charlou et al. (2002).

3. Results

3.1. Decrease of the MgO/SiO_2 ratio in serpentinized peridotites

In MgO/SiO_2 vs. Al_2O_3/SiO_2 diagrams for abyssal peridotites (Fig. 1A), 98% of the serpentinized harzburgites and lherzolites lie under the "terrestrial array" and 85% of the serpentinized dunite have MgO/SiO_2 ratios below 1.2. This corresponds to decreases of the MgO/SiO_2 ratio by 8.1% for harzburgites and lherzolites and by 10.4% for dunites. The lowest MgO/SiO_2 ratios (<0.6) are measured for serpentinized peridotites having experienced Si-metasomatism

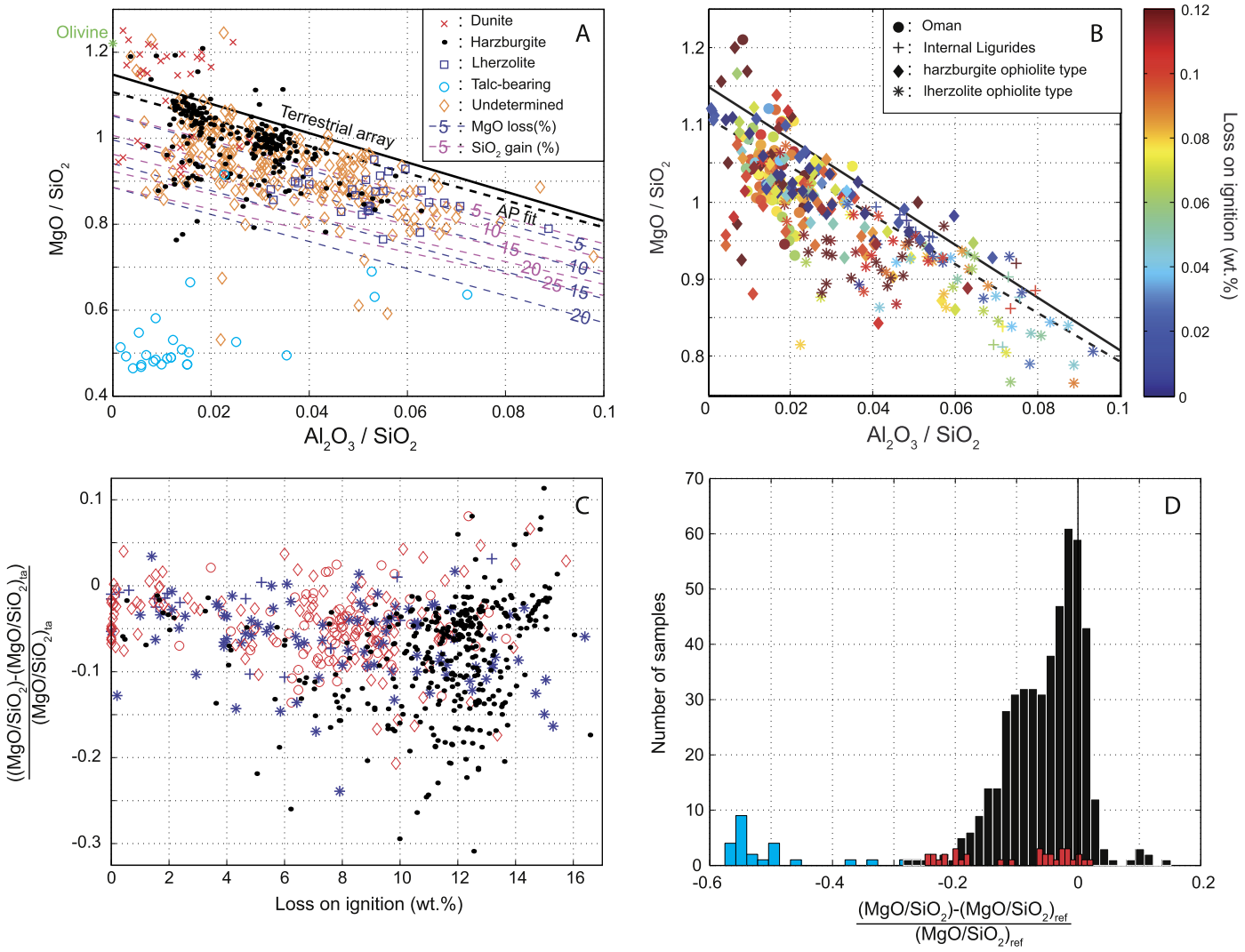

Fig. 1. Compilation of serpentinized peridotite compositions. A: MgO/SiO_2 vs. Al_2O_3/SiO_2 for the compilation of oceanic peridotites (see Supplementary materials Table S1 for references). Different symbols are used depending on the nature of the protolith. The initial compositions of harzburgite and lherzolite are expected to follow the "terrestrial array" (plain line; Jagoutz et al., 1979; Hart and Zindler, 1986) whereas the initial composition of dunite is expected to be close to olivine composition. Line of constant MgO loss (dotted blue lines) and SiO_2 gain (dotted pink lines) are also shown. The data are also compared to the AP fit (dotted black line) for taking into account the influence of other processes than serpentinization on the initial peridotite composition (see text for details). B: MgO/SiO_2 vs. Al_2O_3/SiO_2 for the compilation of ophiolitic harzburgites and lherzolites. The provenance of the samples is indicated with different symbols. The color of the symbols depends on the loss on ignition measured in the samples. The "terrestrial array" (plain line) and the AP fit (dotted line) are also plotted. C: distance from the "terrestrial array" (referred to as ta) as a function of loss on ignition for the harzburgites and lherzolites of the two geochemical datasets. Symbols for the ophiolite samples are the same as in B, the peridotites from harzburgites ophiolite are displayed in red and the peridotites from lherzolite ophiolites are displayed in blue. Data for abyssal peridotites are indicated with black dots. D: distribution of the difference between the MgO/SiO_2 ratio of abyssal peridotites and a reference ratio ($MgO/SiO_{2\,ref}$). This reference ratio was chosen as olivine composition for dunites (red) and AP fit for the harzburgites and lherzolites (black) and for talc-bearing samples (blue). (For interpretation of the references to color in this figure legend, the reader is referred to the web version of this article.)

with talc formation (Paulick et al., 2006; Boschi et al., 2008; Harvey et al., 2014: Fig. 1A).

As discussed in Section 2.1, I used low-LOI, ophiolite peridotite samples from the compilation to determine the deviation from the "terrestrial array" of unaltered abyssal peridotites (Fig. 1B). Samples with LOI below 4 wt.% were found to fall at $3.0 \pm 2.9\%$ below the "terrestrial array" with no clear dependence on the degree of melt depletion (Fig. 1C). A fit of the MgO/SiO_2 vs. Al_2O_3/SiO_2 ratios for these samples gives a slope of 3.145 close to that of 3.406 for the terrestrial array (Fig. 1B and C). In the following, I used this fit (hereafter referred to as AP fit) as a reference for harzburgites and lherzolites having experienced no serpentinization. The few data on abyssal peridotites having LOI below 4 wt.% fall in the same range as the ophiolite data (Fig. 1C). A comparison between this AP fit and the data acquired on abyssal peridotites should provide a quantitative estimate of the impact of serpentinization on mass transfer.

80% of abyssal harzburgite and lherzolite lie below the AP fit with MgO/SiO_2 ratios on average $5.1 \pm 6.1\%$ lower than the fit (Fig. 1D). The measured decrease of the MgO/SiO_2 ratios does not exceed 25% for 99.5% of the harzburgite, lherzolites and dunites (Fig. 1D). The lowest MgO/SiO_2 ratios are measured for the talc-bearing samples with values on average $47 \pm 14\%$ below the one predicted with the AP fit.

3.2. Mineralogical assemblages formed during "isochemical" serpentinization

The "isochemical model" reveals that serpentine, magnetite, brucite and talc are the minerals formed during "isochemical" serpentinization. Here, I focused on the changes in the distribution of Mg and Si between the minerals during serpentinization. For compositions and reaction progresses typical of abyssal peridotites, serpentine is the only Si carrier (Fig. 2). As serpentine and brucite

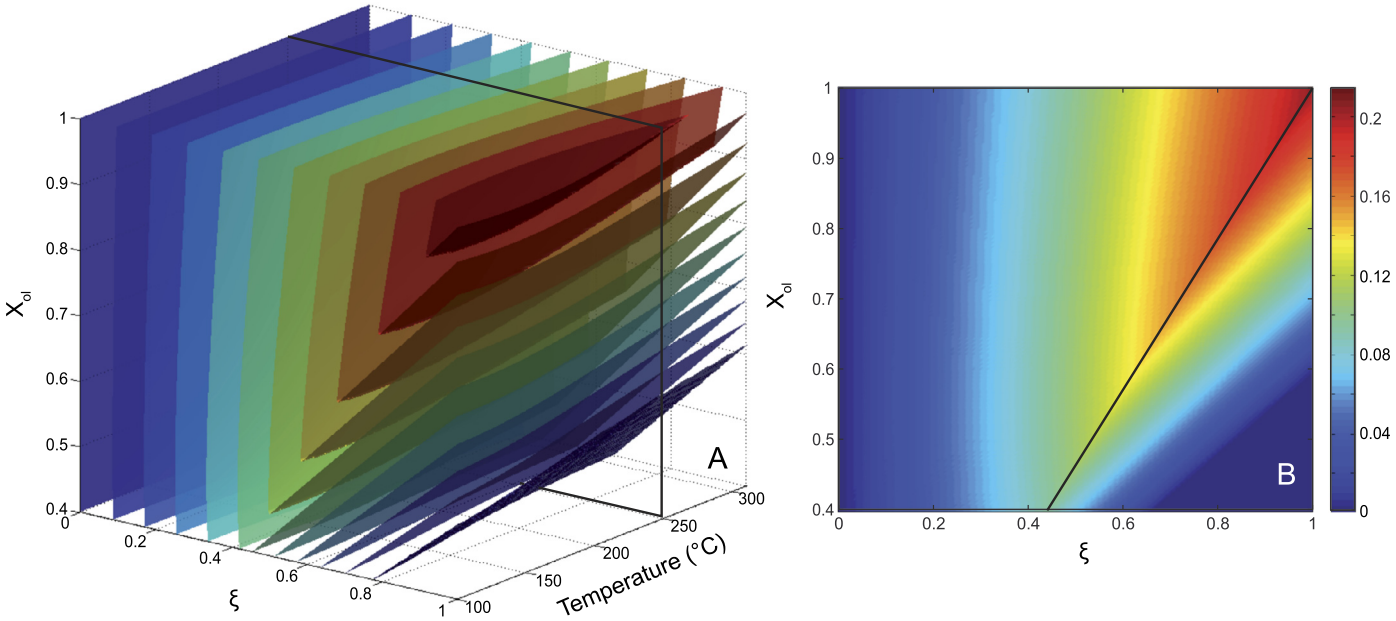

Fig. 2. A: Molar proportion of the Mg in a serpentinized peridotite contained in brucite (X_{Mg}) as a function of temperature, protolith composition (X_{ol} = molar proportion of olivine in a peridotite composed of olivine and orthopyroxene) and reaction progress (ξ). The black line indicates where section B was calculated. B: section across A at a constant temperature of 250 °C. The black line indicated where olivine has been completely consumed.

are the only two carriers of Mg, Mg distribution in the calculations can be inferred with the amount of Mg in brucite and the total amount of Mg in the rock, following $X_{Mg} = Mg_{brucite}/Mg_{rock}$.

The change in the relative reaction rate between olivine and orthopyroxene (r_v) induces changes in the modal composition of the rock. However, these changes are limited to values of r_v below 2 (Fig. S2), i.e., far below the values measured experimentally ($r_v = 14$; Ogasawara et al., 2013). In the following, the value of r_v was thus fixed to 14. The numerical model shows that the distribution of magnesium between the various minerals is mainly dependent on the reaction progress and on the initial composition of the rock rather than on temperature (Fig. 2A).

At 250 °C and for a fixed protolith composition (constant X_{ol}), X_{Mg} first increases with reaction progress up to a value, ξ_{ol}, depending on X_{ol} (Fig. 2B). ξ_{ol} corresponds to the reaction progress where all the olivine contained in the protolith has been consumed, and thus increases with the amount of olivine in the protolith (X_{ol}). Therefore, X_{Mg} reaches its highest value of 20.3 mol.% at 250 °C for a protolith with a dunite composition ($X_{ol} = 1$) at $\xi_{ol} = 1$. For smaller X_{ol} and reaction progresses greater than ξ_{ol}, X_{Mg} progressively decreases. For $X_{ol} < 60$ mol.% at 250 °C, talc can even be produced instead of brucite after complete serpentinization (Fig. 2B).

3.3. Influence of fluid composition and quantity on mass transfer during serpentinization

Fig. 3 shows the influence of the fluid composition, the F/R ratio and the temperature on the mineralogical assemblages formed during the serpentinization of a peridotite having the average composition and reaction progress of the abyssal peridotites. For F/R ratios below ~20 and temperature below 325 °C, the formed mineralogical assemblage is serpentine + brucite + iron carrier with the three fluid compositions. In these conditions, the main iron carrier is magnetite but minor amounts of andradite at F/R ratios below 2 and 20 with seawater and vent fluids, respectively, and wüstite at F/R ratios below 0.4 can also be formed. Hematite formation is observed with MRV fluid and seawater at F/R ratio above ~20 and 60, respectively.

Changes by more than 5% of the MgO/SiO_2 ratio in the solid are only observed at F/R ratios above 10 with vent fluids and $\sim 10^3$ with seawater. Depending on the fluid composition, the MgO/SiO_2 ratio is found to either only decrease or only increase with the F/R ratio for the vent fluids and the seawater, respectively.

When increasing the F/R ratio, the amount of brucite contained in the rock progressively decreases with calculations made with vent fluids (Fig. 3B and C). At F/R ratios of 20 and 100, the only Mg carrier in the rock is serpentine with MRV and URV fluids, respectively. The formed mineralogical assemblage for the average decrease of the MgO/SiO_2 ratio measured in abyssal peridotites lies close to the region where serpentine is the only Mg carrier (Fig. 3E and F). As the F/R ratio increases again, talc formation is predicted. The average MgO/SiO_2 decrease measured in abyssal peridotites having experienced talc alteration is only reproduced with MRV fluids at F/R ratios comprised between 200 and 500 (Fig. 3E).

Decreases in the MgO/SiO_2 ratio comparable with those measured in abyssal peridotites are not calculated when seawater is used as the starting fluid (Fig. 3B). With this fluid composition, ~20 mol.% of talc is also formed with seawater for F/R above 650 but only at temperatures below ~130 °C in the stability field of magnesium-bearing carbonates (dolomite and magnesite; Fig. 3A). For these latter F/R ratios and at higher temperatures, the mineralogical assemblages are dominated by brucite (>50 mol.%).

4. Discussion

4.1. Evidence for mass transfer during serpentinization

Early studies investigated the evolution of oxide ratios during serpentinization in ophiolites and reported very little sensitivity to reaction progress. This was interpreted as indicative of an "isochemical" serpentinization (Coleman and Keith, 1971; Komor et al., 1985). However, small changes in the MgO/SiO_2 ratios were already mentioned by Komor et al. (1985) and conditions prevailing during serpentinization at mid-ocean ridges and in ophiolites are different. Thus, to determine if a change of the MgO/SiO_2 ratio occurs during serpentinization at mid-ocean ridges, samples recovered from the seafloor have to be studied.

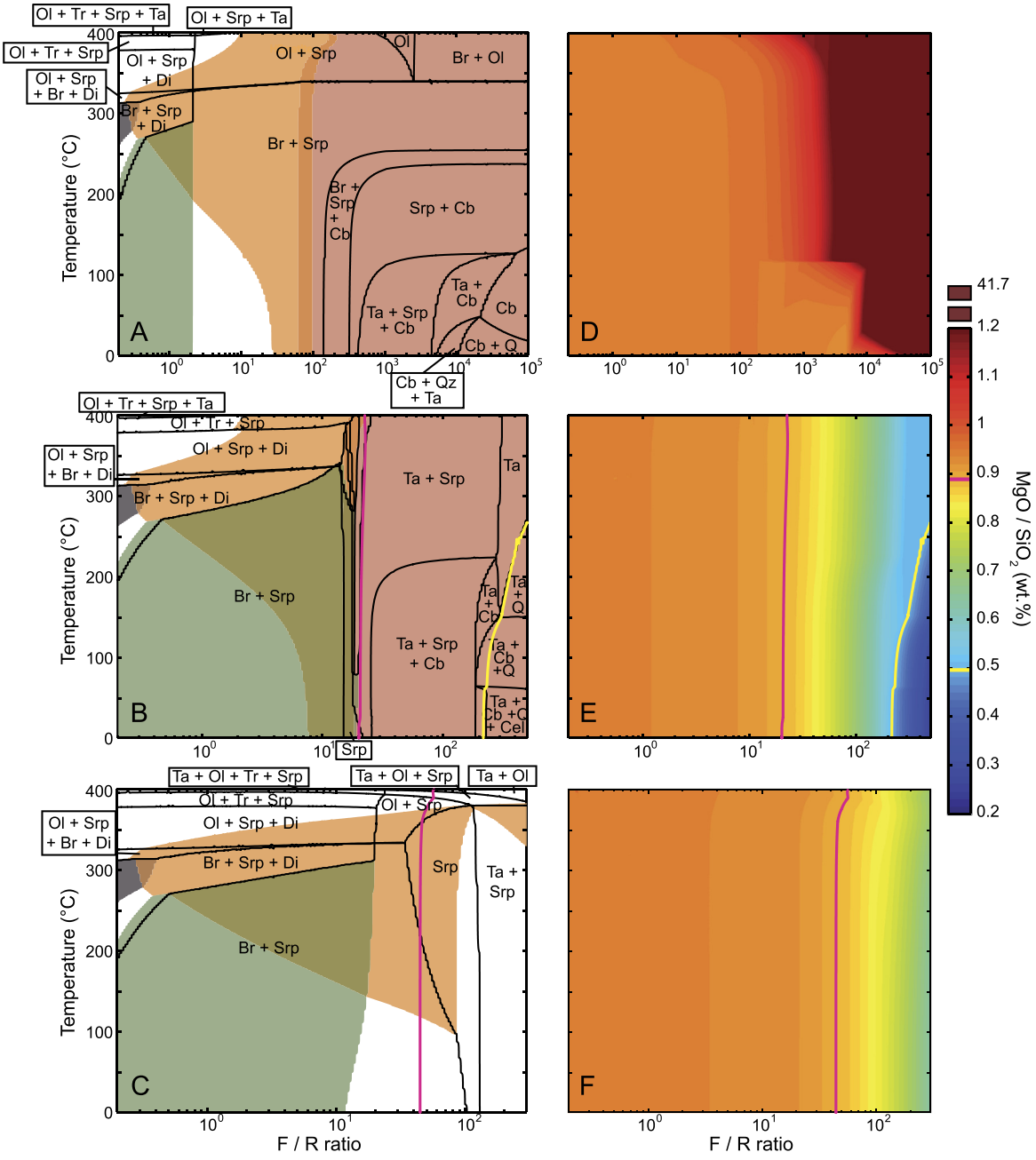

Fig. 3. A, B, C: Calculated mineralogical assemblages at the equilibrium at 50 MPa as a function of temperature and fluid to rock mass ratio for a typical serpentinized peridotite composed of 59.9, 18.6 and 1.5 mol.% of olivine, orthopyroxene and clinopyroxene, respectively, for the reacting part and 18.4 and 1.5 mol.% of orthopyroxene and clinopyroxene, respectively, for the non-reacting part. Fluid compositions of seawater (A), mafic-related vent fluids (B) and ultramafic-related vent fluids (C) were used (see Table 1 for composition). The stability fields of the main iron carriers are represented in colors (wüstite in gray, andradite in green, magnetite in orange and hematite in pink; the fields where two iron carriers are stable are represented with color mixtures). Phases with concentrations below 0.1 mol.% moles are not reported (saponite, nontronite and amesite). Ol: olivine; Srp: serpentine; Di: clinopyroxene; Tr: tremolite; Br: brucite; Cb: carbonate (dolomite or calcite solid solution); Ta: talc; Q: quartz; Cel: céladonite. D, E, F: calculated MgO/SiO_2 ratio for A, B and C, respectively. The pink line corresponds to the mean MgO/SiO_2 measured in oceanic peridotites and the yellow lines to the mean MgO/SiO_2 measured in peridotites having experienced Si-metasomatism with talc alteration. (For interpretation of the references to color in this figure legend, the reader is referred to the web version of this article.)

Abyssal peridotites having experienced an extensive decrease of approximately 50% in their MgO/SiO_2 ratio related to the formation of talc have been reported at the Atlantis Massif (Boschi et al., 2008) and the 15°20′N Fracture zone (Paulick et al., 2006; Harvey et al., 2014). At the 15°20′N Fracture zone, talc alteration was found to be related to a metasomatic event overprinting serpentinization and associated with the percolation of a high temperature SiO_2-rich fluid. As this process is not directly related to mass transfer during serpentinization, samples from Paulick et al. (2006) and Harvey et al. (2014) were not compared to the other samples of our compilation. However, samples from the Atlantis Massif are more relevant for the present study since talc alteration at this site was synchronous with serpentinization (Boschi et al., 2008). The proportion of these latter samples in our compilation does not exceed 2%, suggesting that they only represent end-members resulting from an extreme degree of fluid/rock interaction. For the other more common samples, changes in the average MgO/SiO_2 ratio calculated with samples encompassing the largest possible range of diversity (i.e. reaction progress, location and serpentinization conditions) have to be investigated since compositional changes are expected to be small.

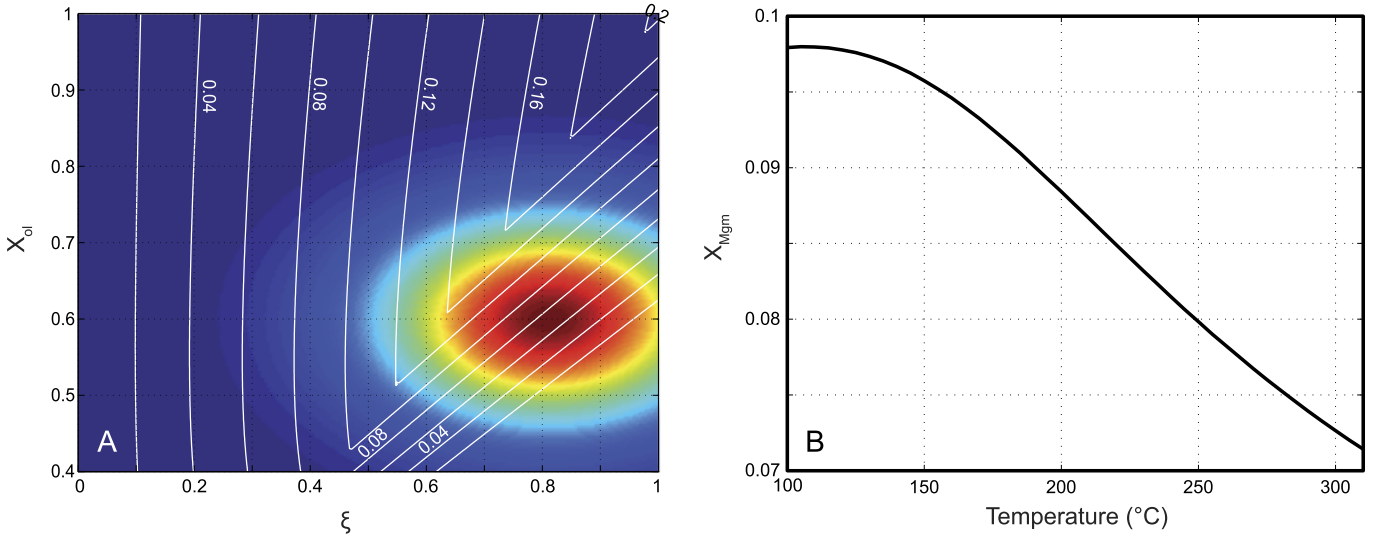

Fig. 4. Determination of the average amount of Mg contained in brucite (X_{Mgm}) in a peridotite having the average molar olivine content ($X_{olm} = 62 \pm 9.5\%$, Niu, 2004) and having experienced "isochemical" serpentinization with the average reaction progress ($\xi_m = 80 \pm 20\%$; Cannat et al., 2010) of abyssal peridotites. A: bivariate Gaussian distribution (f) of the abyssal peridotites determined with ξ_m and X_{olm}. The white lines are the calculated X_{Mg} at 250 °C (see Fig. 2 for details). B: X_{Mgm} as a function of temperature. X_{Mgm} was calculated as follows: $X_{Mgm} = \frac{\iint (X_{Mg}(\xi, X_{ol}) f(\xi, X_{ol})) d\xi dX_{ol}}{\iint f(\xi, X_{ol}) d\xi dX_{ol}}$.

Snow and Dick (1995) and Niu (2004) reported a decrease of the average MgO/SiO_2 ratio by approximately 10% in abyssal peridotites. However, they attributed this decrease not to serpentinization itself but to alteration on the seafloor by seawater below 100 °C through brucite dissolution and incongruent olivine dissolution preferentially releasing Mg cations in seawater. In the present study, a decrease of the MgO/SiO_2 by 8%, close to the one measured by Niu (2004) was measured when comparing abyssal peridotites to the "terrestrial array". However, samples having experienced limited serpentinization (LOI < 4%) indicate that 3% of the change in MgO/SiO_2 is due to a deviation of unaltered abyssal peridotites composition from the "terrestrial array". The remaining 5% of the total MgO/SiO_2 ratio decrease must be related to mass transfer during serpentinization.

4.2. Mechanism of mass transfer during serpentinization

Thermodynamic modeling and observations in natural samples suggest that "isochemical" serpentinization follows a reaction path where olivine first reacts at low activity in silica ($aSiO_2$) to form serpentine and brucite. Then $aSiO_2$ in the fluid progressively increases due to pyroxene breakdown occurring slower than olivine breakdown at $T < 350$ °C and brucite reacts to form serpentine (Bach et al., 2004; Ogasawara et al., 2013). This latter process is favored by an easy access of high $aSiO_2$ fluids to brucite, which precipitates in the core of serpentine veins in both mid-ocean ridge dunites and in experiments (Plümper et al., 2012; Malvoisin and Brunet, 2014). Complete serpentinization of a peridotite with the average composition of abyssal peridotites ($X_{ol} =$ 60%) should therefore produce only serpentine as reaction product (Fig. 2). Similar results were used to explain why brucite is only rarely observed in serpentinized peridotites (Klein et al., 2009; Klein et al., 2013). Brucite has only been observed at locations where dunite has also been described: the 15°20′N Fracture Zone (Bach et al., 2004; Paulick et al., 2006; Klein et al., 2009; Kodolányi et al., 2012), the MARK area (Dilek et al., 1997; Alt and Shanks, 2003), the Atlantis Massif (Beard et al., 2009) and the Hess Deep area (Gillis et al., 1993). However, estimates of the amount of brucite formed during complete serpentinization of abyssal dunites (D'Antonio and Kristensen, 2004) are approximately 10% lower than the one determined here with the "isochemical" model. Moreover, abyssal peridotites are generally not completely serpentinized and, for the mean composition and reaction progress of abyssal peridotites ($X_{ol} = 60\%$ and $\xi = 80$ mol.%), brucite should be produced (Fig. 2). Using a bivariate normal distribution of abyssal peridotites (Fig. 4A), the mean X_{Mg} for "isochemical" serpentinization is estimated to vary between 7.8 and 10.4% for temperature of 100 °C and 310 °C, respectively (Fig. 4B). These values are comparable to the decrease of the MgO/SiO_2 ratio of $5.1 \pm 6.1\%$ measured in the geochemical data compilation. The decrease of the MgO/SiO_2 ratio thus appears to be related to the scarcity of brucite in serpentinized peridotites.

Two mechanisms can jointly account for the decrease of the MgO/SiO_2 ratio and the scarcity of brucite in serpentinized peridotites: 1) Mg loss through brucite dissolution (Snow and Dick, 1995):

$$Mg(OH)_2 = Mg^{2+} + 2OH^- \quad (1)$$

or 2) SiO_2 gain through the reaction with high $aSiO_2$ fluids to form serpentine with or without brucite as a reaction intermediate (Beard et al., 2009; Frost et al., 2013):

$$3Mg^{2+} + 6OH^- + 2SiO_{2,aq} = 3Mg(OH)_2 + 2SiO_{2,aq} = Mg_3Si_2O_5(OH)_4 + H_2O \quad (2)$$

$$\Delta V_s = (V_{m\ \text{serpentine}} - 3V_{m\ \text{brucite}})/(3V_{m\ \text{brucite}}) = 47\%$$

(The volume change of the solid ($\Delta V_s = (V_{\text{solid products}} - V_{\text{solid reactants}})/V_{\text{solid reactants}}$) is given here and for the reactions below, and will be further discussed in Section 4.3.1.)

Mechanism of brucite dissolution was not reproduced with thermodynamic modeling even with seawater, low temperature and high F/R ratios as proposed by Snow and Dick (1995) (Fig. 3). On the contrary, brucite was found to precipitate with carbonate in these conditions from the Mg contained in seawater (Fig. 3A). This mineralogical composition is the same as the one observed in the hydrothermal chimneys of the Lost City hydrothermal field (Kelley et al., 2001). These results are consistent with experiments of peridotite serpentinization in which Mg was transferred from seawater to peridotite at temperatures of 200 °C and F/R ratio of ~1 (Seyfried et al., 2007) and not from peridotite to seawater.

A decrease of the MgO/SiO_2 ratio was obtained with the MRV and URV fluids containing aqueous silica (Fig. 3E and F). As the F/R

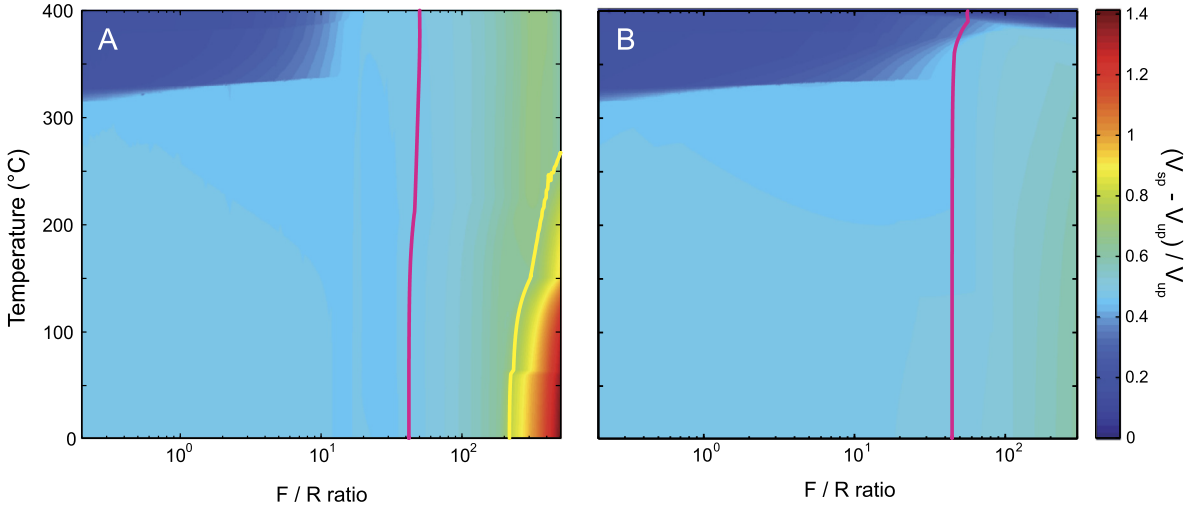

Fig. 5. Solid volume change as a function of temperature and fluid to rock ratio calculated with MRV (A) and URV fluid (B). The same composition as in Fig. 3 is used for the protolith. The pink line represents the calculated position of the average composition of abyssal peridotites, the yellow line shows the calculated position of the average composition of abyssal peridotites having experienced extreme Si-metasomatism with talc alteration. (For interpretation of the references to color in this figure legend, the reader is referred to the web version of this article.)

ratio increases, brucite was found to be only stable below F/R ratios of 20 and 100 for MRV and URV fluids, respectively. At these F/R ratios, a mineralogical composition typical of abyssal peridotites with serpentine and magnetite as main minerals was obtained with corresponding decreases of the MgO/SiO_2 ratio around 5%, i.e. in the same range as that measured in abyssal peridotites. At higher F/R ratios, talc was found to precipitate directly from aqueous species or with serpentine as an intermediate of reaction:

$$3Mg^{2+} + 6OH^- + 4SiO_{2,aq} = Mg_3Si_2O_5(OH)_4 + 2SiO_{2,aq} + H_2O$$
$$= Mg_3Si_4O_{10}(OH)_2 + 2H_2O$$
$$\Delta V_s = (V_{m\,\mathrm{talc}} - V_{m\,\mathrm{serpentine}})/(V_{m\,\mathrm{serpentine}}) = 26\% \quad (3)$$

This reaction induces pronounced decreases of the MgO/SiO_2 ratio and is compatible with the observation of talc-bearing rocks (Boschi et al., 2008). Mass transfer during serpentinization can thus be explained by fluid/rock interactions with SiO_2-rich fluids leading to the formation of serpentine (reaction (2)) or talc (reaction (3)). Most of the serpentinized peridotites have only experienced reaction (2) indicating F/R ratios comprised between 20 and 50, i.e., in the range calculated from isotopic measurements by Delacour et al. (2008), but orders of magnitude smaller than that determined by Snow and Reisberg (1995) with osmium isotopes.

It is difficult to determine if MRV fluid, URV fluid or both fluids are the source of aqueous silica in natural systems since they all yielded similar results. Moreover, Si mobilization during hydrothermal alteration of mafic bodies at temperatures ranging from 70 to 300 °C and of ultramafic bodies at 400 °C have both been reported in the literature (Seyfried and Mottl, 1982; Seyfried and Bischoff, 1979; Allen and Seyfried, 2003). The formation of hematite with MRV fluids at high F/R ratios is compatible with observations of talc-bearing samples showing evidence of Si transfer from mafic to ultramafic rocks (Paulick et al., 2006). The presence of mafic intrusions in exhumed mantle rocks (e.g., Cannat, 1993) thus plays a key role in Si transfer during serpentinization not only for 2% of the samples recovered at mid-ocean ridges having experienced extreme alteration in the vicinity of gabbroic rocks (Boschi et al., 2008), but also for more than 80% of the abyssal peridotites. The modeling performed here indicates that the formation of talc-bearing rocks is not necessary a two-stage process during which serpentinized peridotites are first formed and then altered with high $aSiO_2$ fluids (Paulick et al., 2006; Harvey et al., 2014), but can also be a single-step process of serpentinization with high $aSiO_2$ fluids and high F/R ratios (Boschi et al., 2008).

4.3. Consequences of mass transfer during serpentinization

4.3.1. Estimating volume change of reaction

"Isochemical" serpentinization is known to be associated with a positive ΔV_s of up to 40% (ΔV_s; Coleman and Keith, 1971). This increase can have two opposite consequences for fluid transport during serpentinization. On the one hand, it can generate a pressure build-up susceptible of fracturing the peridotite and propagating fluids inwards (e.g. Plümper et al., 2012). On the other hand, the expanding reaction products can fill the porosity and lower permeability, preventing efficient fluid transport through the rock (Godard et al., 2013). An estimate of the influence of Si metasomatism during serpentinization on ΔV_s was obtained by using the "open system" model (Fig. 5). ΔV_s was found to be rather constant around 50% for F/R ratios below 100, i.e., in the domain where serpentinized peridotites with the average composition of abyssal peridotites are expected to form (Fig. 3). This constant value of ΔV_s is due to a competition between the transformation of brucite into serpentine (reaction (2)), which is associated with a solid volume increase, and the formation of high-density magnetite from low density Fe-brucite:

$$3Fe(OH)_2 = Fe_3O_4 + 2H_2O + H_2 \quad (4)$$
$$\Delta V_s = (V_{m\,\mathrm{magnetite}} - 3V_{m\,\mathrm{Fe\text{-}brucite}})/(3V_{m\,\mathrm{Fe\text{-}brucite}})$$
$$= -44\% \quad (5)$$

For F/R ratios above 100, ΔV_s significantly increases and values of approximately 70% are obtained for the average composition of abyssal peridotites having experienced extreme Si-metasomatism (Fig. 5A). This sharp increase is associated with volume increase during talc formation (reaction (3)). Serpentinization at mid-ocean ridges is therefore associated with significant solid volume increases. This said, understanding the mechanisms of porosity generation before (e.g. tectonic deformation, thermal cracking) or during serpentinization (e.g. reaction-induced fracturing) remains a major challenge.

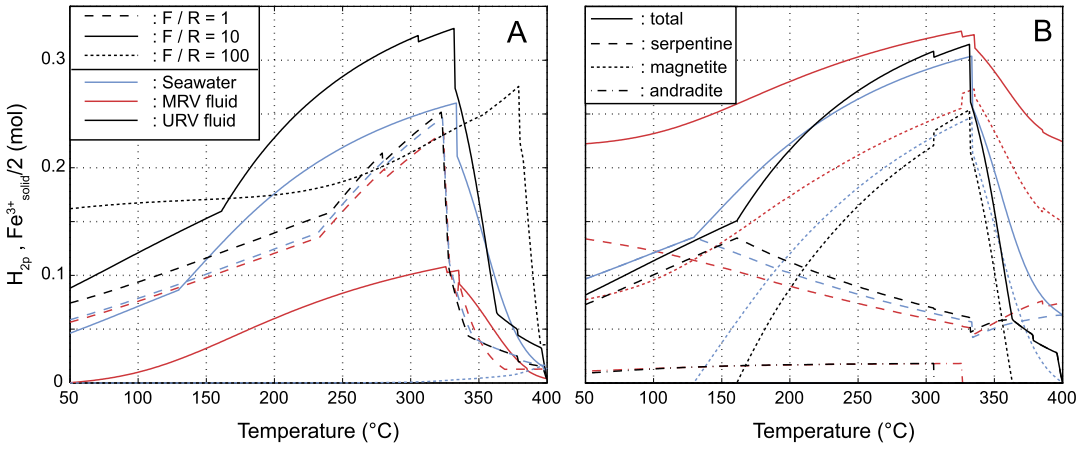

Fig. 6. Dependence of the amount of hydrogen produced (H_{2p}) on the F/R ratio and the initial fluid composition. A: H_{2p} as a function of temperature for the seawater, MRV and URV fluids at F/R ratio of 1, 10 and 100. B: number of moles of Fe^{3+} divided by 2 in serpentine, magnetite, andradite and in the solid as a function of temperature. The same labels as in Fig. 6A are used for the color of the lines. (For interpretation of the references to color in this figure legend, the reader is referred to the web version of this article.)

4.3.2. Hydrogen production

Serpentinization is a redox reaction producing hydrogen through two coupled half-reactions of water reduction and iron oxidation during magnetite and serpentine formation (Charlou et al., 2002):

$$2Fe^{2+}_{(\text{olivine, pyroxene})} = 2Fe^{3+}_{(\text{magnetite, serpentine})} + 2e^- \quad (6)$$

$$2H_2O + 2e^- = H_2 + 2OH^-_{(\text{brucite, serpentine, talc})} \quad (7)$$

Hydrogen is an energy source for both biological organisms and human activities (Früh-Green et al., 2003; Malvoisin et al., 2013). Identifying the parameters controlling the amount of hydrogen produced during serpentinization therefore has major scientific and societal implications. Thermodynamic models have established that temperature and reacting peridotite composition are two of these parameters (Klein et al., 2013). The "open system" model used here suggests that the F/R ratio and the fluid composition are also key parameters (Fig. 6). However, increasing the F/R ratio can produce opposite trends in the total amount of produced hydrogen (H_{2p}) with different fluid compositions and there is thus no simple relationship between the F/R ratio and H_{2p} or between the fluid composition and H_{2p}. For example, at a F/R ratio of 100, hydrogen is only produced with the URV fluid. This is directly related to the fluid composition since, at this F/R ratio with the high Si content in MRV fluid and the high Mg content in seawater (Table 1), rocks are composed of iron in its reduced form (Fe^{2+}), which is carried by talc and brucite (Figs. 3 and 7B). Changing from a F/R ratio of 1 to a F/R ratio of 10 produces different H_{2p} depending on the fluid composition. Due to a dilution effect, this change leads to lower hydrogen concentrations in the fluid. With seawater and URV fluid, the dilution effect is responsible for higher H_{2p}, since higher amount of hydrogen can be dissolved in the fluid before reaching thermodynamic equilibrium. However, this effect is counterbalanced by the occurrence of other half-reactions besides (7) to equilibrate (6), resulting in oxidation of the solid (Fig. 6B) without hydrogen production (Fig. 6A). Detailed investigation of the amount of the various aqueous species as a function of the F/R ratio (Fig. S3 in Supplementary materials) reveals that the reduction of $O_{2,aq}$ is one of these reactions:

$$O_{2,aq} + 2H_2O + 4e^- = 4OH^- \quad (8)$$

Hydrogen can also be consumed during reactions with aqueous species such as HCO^{3-}_{aq} to form potassium acetate (Fig. S3):

$$2HCO_3^- + K^+ + OH^- + 5H_2 = K(CH_3COO)^{2-} + 5H_2O. \quad (9)$$

The effect of these reactions on H_{2p} is more pronounced at higher F/R ratios since the total amount of $O_{2,aq}$ and HCO^{3-}_{aq} also increases with F/R ratio. That is why comparable H_{2p} are obtained with the three fluids for a F/R of 1. Consequently, determining the exact composition and the amount of fluid involved during serpentinization is essential for providing accurate estimates of H_{2p}.

4.3.3. Fluid release in subduction zones

At slow and ultraslow spreading ridges, mantle-derived ultramafic rocks are estimated to represent approximately 9% of the oceanic crust and are produced at a rate of 0.4 km^3/yr (Cannat et al., 2010). Therefore, mass transfers in mantle rocks have the potential to induce large changes in seawater composition. In particular, calculations performed by Snow and Dick (1995) and Ligi et al. (2013) indicate that a MgO/SiO_2 ratio decrease in serpentinized peridotites resulting from Mg loss during weathering can contribute to the Mg content of seawater to a level similar to the input from rivers. Here, the decrease in MgO/SiO_2 ratio is reinterpreted as resulting mainly from a process implying a Si gain through serpentinization with Si-rich fluids. During this process, minerals with progressively smaller H_2O/Mg ratios (X_{H_2O}) are produced as more Si is incorporated in the rock (Fig. 7). This leads to serpentine and talc having X_{H_2O} of 2/3 and 1/3, while brucite has a X_{H_2O} of 1. Compared to "isochemical" serpentinization, this induces an incorporation of water that can be 13 to 70% lower when serpentine and talc are formed, respectively (Fig. 7).

The changes in composition associated with Si-metasomatism during serpentinization on the seafloor could also have consequences on the pressure and temperature at which water is released in subduction zones. To quantify this effect, another thermodynamic model appropriate for subduction zone conditions was built with Perple_X (Connolly, 2005). The amount of water released along a slab interface with a thermal gradient of 10 °C/km was estimated for three different serpentinized peridotite compositions determined with the "open system" model during peridotite/MRV fluid interaction at 250 °C. To investigate different degrees of Si-metasomatism, the three compositions were extracted from the model at F/R ratios of 1, 30 and 400, which are assumed to reproduce 1) the conditions of "isochemical" serpentinization (IS peridotites; SiO_2 = 44.6 wt.% on an anhydrous basis), 2) Si-metasomatism experienced by most of the abyssal peridotites (NSi peridotites; SiO_2 = 46.3 wt.% on an anhydrous basis), and 3) extreme Si-metasomatism with talc alteration (ESi peridotites; SiO_2 = 57.4 wt.% on an anhydrous basis), respectively. Fig. 8 indicates that the release of water by IS peridotites occurs in two steps at ~440 °C/1.3 GPa and 610 °C/1.8 GPa corresponding to brucite

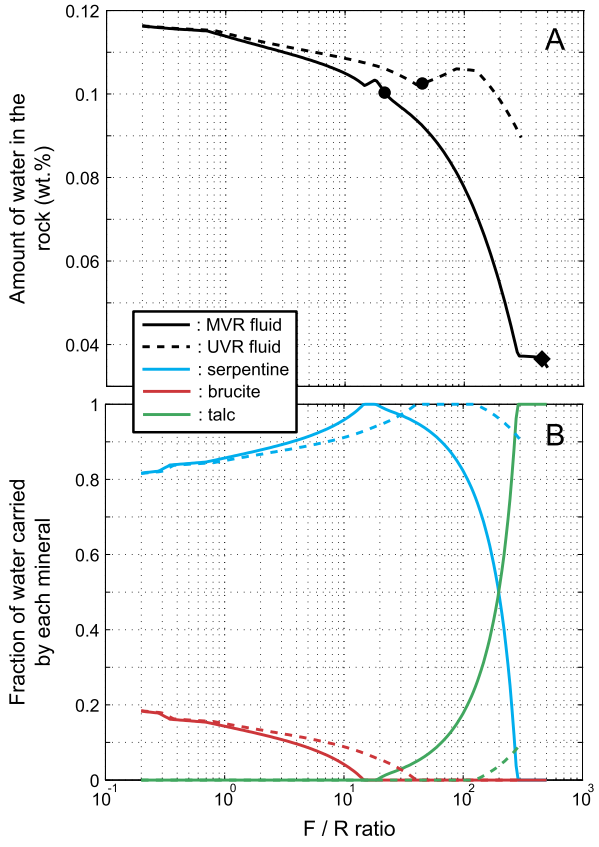

Fig. 7. A: amount of water contained in the rock as a function of the fluid to rock ratio at 250 °C for two initial fluid compositions (MRV and URV fluids). The black dots are the points where the average composition of abyssal peridotites is calculated and the black diamond is the point where the average composition of abyssal peridotites having experienced extreme Si-metasomatism with talc alteration is calculated. B: number of moles of water on total amount of water in serpentine, brucite and talc as a function of the fluid to rock ratio at 250 °C calculated with MRV and URV fluids.

and serpentine dehydrations, respectively, whereas NSi peridotites only experience serpentine dehydration at an unique pressure of ∼650 °C/1.9 GPa. The dehydration of talc-bearing ESi peridotites even occurs at higher pressure since dry peridotites formed after ESi peridotites are only found at pressures above 750 °C/2.2 GPa. These results suggest that Si-metasomatism is responsible for a shifting of the water release in subduction zones by more than 0.6 GPa, i.e. 20 km depth assuming a lithostatic pressure in the rock column. These results must be taken into account when modeling the impact of serpentinized peridotites dehydration on fluid release in the mantle wedge at subduction zones.

5. Conclusion

A compilation of ∼500 abyssal peridotites compositions reveals a systematic decrease of the MgO/SiO_2 ratio by 5% on average relative to unaltered peridotites. Additionally, brucite is not commonly observed in serpentinized peridotites even though thermodynamic modeling of "isochemical" serpentinization predicts that this mineral should represent ∼40 mol.% of the mineralogical assemblage. These two observations were only reproduced numerically during peridotite interaction with Si-rich fluids inducing serpentine production at F/R ratios of ∼20 and talc production at higher F/R ratios. These results extend the model of Boschi et al. (2008) of peridotite serpentinization with Si-rich fluids produced during mafic rocks alteration from talc-bearing samples to 80% of abyssal peridotites. Compared to "isochemical" serpentinization, this process of SiO_2 gain during serpentinization also reduces the amount

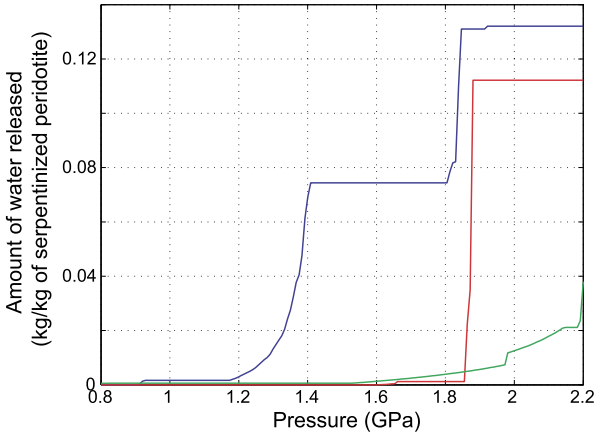

Fig. 8. Mass of water released along a metamorphic gradient of 10 °C/km (T (K) = 298 + 0.003P (MPa)). The input compositions of the serpentinized peridotites were obtained with the "open system" model (Fig. 3) at 250 °C with the MRV fluid and F/R ratio of 1 (blue line; MgO/SiO_2 = 1.034), 30 (red line; MgO/SiO_2 = 0.942) and 400 (black line; MgO/SiO_2 = 0.387). The corresponding initial mineralogical assemblages are serpentine + brucite + andradite + magnetite for F/R ratio of 1, serpentine + talc + hematite for F/R ratio of 30 and talc + hematite for F/R ratio of 400. (For interpretation of the references to color in this figure legend, the reader is referred to the web version of this article.)

of hydrogen produced at mid-ocean ridges and increases the depth at which water is released through the dehydration of serpentinized peridotites in subduction zones. However, it has a limited impact on volume increase during serpentinization since serpentinized peridotites have a constant ∼1.5 times greater volume than unaltered peridotites for F/R ratios below 100.

Acknowledgements

I thank Mathilde Cannat, Catherine Mével and Fabrice Brunet for insightful discussions. I also thank Frieder Klein and Thomas McCollom for providing the database that was used for thermodynamic modeling. I gratefully acknowledge two anonymous reviewers for their constructive comments that helped to significantly improve the manuscript. I am also grateful to Jean-Arthur Olive for correcting the English of this manuscript. Chiara Boschi is thanked for providing data for the Al_2O_3 content in samples from the Atlantis Massif

Appendix A. Supplementary material

Supplementary material related to this article can be found online at http://dx.doi.org/10.1016/j.epsl.2015.07.043.

References

Allen, D.E., Seyfried Jr., W.E., 2003. Compositional controls on vent fluids from ultramafic-hosted hydrothermal systems at mid-ocean ridges: an experimental study at 400 °C, 500 bars. Geochim. Cosmochim. Acta 67, 1531–1542.

Alt, J.C., Shanks, W.C., 2003. Serpentinization of abyssal peridotites from the MARK area, Mid-Atlantic Ridge: sulfur geochemistry and reaction modeling. Geochim. Cosmochim. Acta 67, 641–653.

Andreani, M., Mével, C., Boullier, A.-M., Escartin, J., 2007. Dynamic control on serpentine crystallization in veins: constraints on hydration processes in oceanic peridotites. Geochem. Geophys. Geosyst. 8, 1–24.

Bach, W., Garrido, C.J., Paulick, H., Harvey, J., Rosner, M., 2004. Seawater-peridotite interactions: first insights from ODP Leg 209, MAR 15°N. Geochem. Geophys. Geosyst. 5, 1–22.

Beard, J.S., Frost, B.R., Fryer, P., McCaig, A., Searle, R., Ildefonse, B., Zinin, P., Sharma, S.K., 2009. Onset and progression of serpentinization and magnetite formation in olivine-rich troctolite from IODP Hole U1309D. J. Petrol. 50, 387–403.

Bodinier, J.-L., Godard, M., 2003. Orogenic, ophiolitic, and abyssal peridotites. In: Carlson, R.W. (Ed.), Mantle and Core. In: Treatise on Geochemistry, vol. 2. Elsevier Science Ltd., pp. 103–170.

Boschi, C., Dini, A., Früh-Green, G.L., Kelley, D.S., 2008. Isotopic and element exchange during serpentinization and metasomatism at the Atlantis Massif (MAR 30°N): insights from B and Sr isotope data. Geochim. Cosmochim. Acta 72, 1801–1823.

Canales, J.P., Collins, J.A., Escartin, J., Detrick, R.S., 2000. Seismic structure across the rift valley of the Mid-Atlantic ridge at 23°20′N (MARK area): implications for crustal accretion processes at slow-spreading ridges. J. Geophys. Res. 105, 28411–28425.

Cannat, M., 1993. Emplacement of mantle rocks in the seafloor at mid-ocean ridges. J. Geophys. Res. 98, 4163–4172.

Cannat, M., Fontaine, F., Escartin, J., 2010. Serpentinization and associated hydrogen and methane fluxes at slow spreading ridges. In: Rona, P.A. (Ed.), Diversity of Hydrothermal Systems on Slow Spreading Ocean Ridges. In: Geophysical Monograph Series, pp. 241–264.

Charlou, J.L., Donval, J.P., Fouquet, Y., Jean-Baptiste, P., Holm, N., 2002. Geochemistry of high H_2 and CH_4 vent fluids issuing from ultramafic rocks at the Rainbow hydrothermal field (36°14′N, MAR). Chem. Geol. 191, 345–359.

Coleman, R.G., Keith, T.E., 1971. A chemical study of serpentinization – Burro Mountain, California. J. Petrol. 12, 311–328.

Connolly, J.A.D., 2005. Computation of phase equilibria by linear programming: a tool for geodynamic modeling and its application to subduction zone decarbonation. Earth Planet. Sci. Lett. 236, 524–541.

D'Antonio, M., Kristensen, M.B., 2004. Serpentine and brucite of ultramafic clasts from the South Chamorro Seamount (Ocean Drilling Program Leg 195, Site 1200): inferences for the serpentinization of the Mariana forearc mantle. Mineral. Mag. 68, 887–904.

Delacour, A., Früh-Green, G.L., Frank, M., Gutjahr, M., Kelley, D.S., 2008. Sr- and Nd-isotope geochemistry of the Atlantis Massif (30°N, MAR): implications for fluid fluxes and lithospheric heterogeneity. Chem. Geol. 254, 19–35.

Deschamps, F., Godard, M., Guillot, S., Hattori, K., 2013. Geochemistry of subduction zone serpentinites: a review. Lithos 178, 96–127.

Dilek, Y., Coulton, A., Hurst, S.D., 1997. Serpentinization and hydrothermal veining in peridotites at Site 920 in the MARK area. In: Proceedings of the Ocean Drilling Program, Scientific Results, vol. 153, pp. 35–59.

Escartín, J., Hirth, G., Evans, B., 2001. Strength of slightly serpentinized peridotites: implications for tectonics of oceanic lithosphere. Geology 29, 1023–1026.

Frost, B.R., Evans, K.A., Swapp, S.M., Beard, J.S., Mothersole, F.E., 2013. The process of serpentinization in dunite from New Caledonia. Lithos 178, 24–39.

Früh-Green, G.L., Kelley, D.S., Bernasconi, S.M., Karson, J.A., Ludwig, K.A., Butterfield, D.A., Boschi, C., Proskurowski, G., 2003. 30,000 years of hydrothermal activity at the Lost City vent field. Science 301, 495–498.

Gillis, K., Mével, C., Allan, J., et al., 1993. Site 895. In: Proceedings of the Ocean Drilling Program, Initial Reports, vol. 147, pp. 109–159.

Godard, M., Luquot, L., Andreani, M., Gouze, P., 2013. Incipient hydration of mantle lithosphere at ridges: a reactive-percolation experiment. Earth Planet. Sci. Lett. 371, 92–102.

Hart, S.R., Zindler, A., 1986. In search of bulk Earth composition. Chem. Geol. 57, 247–267.

Harvey, J., Savov, I.P., Agostini, S., Cliff, R.A., Walshaw, R., 2014. Si-metasomatism in serpentinized peridotite: the effects of talc-alteration on strontium and boron isotopes in abyssal serpentinites from Hole 1268a, ODP Leg 209. Geochim. Cosmochim. Acta 126, 30–48.

Jagoutz, E., Palme, H., Blum, H., Cendales, M., Dreibus, G., Spettel, B., Lorenz, V., Wänke, H., 1979. The abundances of major, minor and trace elements in the Earth's mantle as derived from primitive ultramafic nodules. In: Proceedings of 10th Lunar Planetary Science Conference. In: Geochim. Cosmochim. Acta, Suppl., vol. 10, pp. 2031–2051.

Kelley, D.S., Karson, J.A., Blackman, D.K., Früh-Green, G.L., Butterfield, D.A., et al., 2001. An off-axis hydrothermal vent field near the Mid-Atlantic ridge at 30°N. Nature 412, 145–149.

Klein, F., Bach, W., Jöns, N., McCollom, T., Moskowitz, B., Berquó, T., 2009. Iron partitioning and hydrogen generation during serpentinization of abyssal peridotites from 15°N on the Mid-Atlantic Ridge. Geochim. Cosmochim. Acta 73, 6868–6893.

Klein, F., Bach, W., McCollom, T.M., 2013. Compositional controls on hydrogen generation during serpentinization of ultramafic rocks. Lithos 178, 55–69.

Kodolányi, J., Pettke, T., Spandler, C., Kamber, B.S., Gméling, K., 2012. Geochemistry of ocean floor and fore-arc serpentinites: constraints on the ultramafic input to subduction zones. J. Petrol. 53, 235–270.

Komor, S.C., Elthon, D., Casey, J.F., 1985. Mineralogic variation in a layered ultramafic cumulate sequence at the North Arm Mountain Massif, Bay of Islands ophiolite, Newfoundland. J. Geophys. Res. 90, 7705–7736.

Ligi, M., Bonatti, E., Cuffaro, M., Brunelli, D., 2013. Post-mesozoic rapid increase of seawater Mg/Ca due to enhanced mantle-seawater interaction. Sci. Rep. 3.

Malvoisin, B., Brunet, F., 2014. Water diffusion-transport in a synthetic dunite: consequences for oceanic peridotite serpentinization. Earth Planet. Sci. Lett. 403, 263–272.

Malvoisin, B., Carlut, J., Brunet, F., 2012a. Serpentinization of oceanic peridotites: 1. A high-sensitivity method to monitor magnetite production in hydrothermal experiments. J. Geophys. Res., Solid Earth 117.

Malvoisin, B., Brunet, F., Carlut, J., Rouméjon, S., Cannat, M., 2012b. Serpentinization of oceanic peridotites: 2. Kinetics and processes of San Carlos olivine hydrothermal alteration. J. Geophys. Res. 117, B04102.

Malvoisin, B., Brunet, F., Carlut, J., Montes-Hernandez, G., Findling, N., Lanson, M., Vidal, O., Bottero, J.-Y., Goffé, B., 2013. High-purity hydrogen gas from the reaction between BOF steel slag and water in the 473–673 K range. Int. J. Hydrog. Energy 38, 7382–7393.

Mével, C., 2003. Serpentinization of abyssal peridotites at mid-ocean ridges. C. R. Géosci. 335, 825–852.

Miller, D.J., Christensen, N.I., 1997. Seismic velocities of lower crustal and upper mantle rocks from the slow-spreading mid-Atlantic ridge, south of the Kane Transform zone (MARK). In: Proceedings of the Ocean Drilling Program, Scientific Results, vol. 153, pp. 437–454.

Niu, Y., 2004. Bulk-rock major and trace element compositions of abyssal peridotites: implications for mantle melting, melt extraction and post-melting processes beneath mid-ocean ridges. J. Petrol. 45, 2423–2458.

Niu, Y., Langmuir, C.H., Kinzler, R.J., 1997. The origin of abyssal peridotites: a new perspective. Earth Planet. Sci. Lett. 152, 251–265.

Ogasawara, Y., Okamoto, A., Hirano, N., Tsuchiya, N., 2013. Coupled reactions and silica diffusion during serpentinization. Geochim. Cosmochim. Acta 119, 212–230.

Paulick, H., Bach, W., Godard, M., De Hoog, J.C.M., Suhr, G., Harvey, J., 2006. Geochemistry of abyssal peridotites (15°20′N, ODP Leg 209): implications for fluid/rock interaction in slow spreading environments. Chem. Geol. 234, 179–210.

Plümper, O., Røyne, A., Magrasó, A., Jamtveit, B., 2012. The interface-scale mechanism of reaction-induced fracturing during serpentinization. Geology 40, 1103–1106.

Schwarzenbach, E.M., Frueh-Green, G.L., Bernasconi, S.M., Alt, J.C., Plas, A., 2013. Serpentinization and carbon sequestration: a study of two ancient peridotite-hosted hydrothermal systems. Chem. Geol. 351, 115–133.

Seyfried Jr., W.E., Bischoff, J.L., 1979. Low temperature basalt alteration by seawater: an experimental study at 70 °C and 150 °C. Geochim. Cosmochim. Acta 43, 1937–1947.

Seyfried Jr., W.E., Mottl, M.J., 1982. Hydrothermal alteration of basalt by seawater under seawater-dominated conditions. Geochim. Cosmochim. Acta 46, 985–1002.

Seyfried Jr., W.E., Foustoukos, D.I., Fu, Q., 2007. Redox evolution and mass transfer during serpentinization: an experimental and theoretical study at 200 °C, 500 bar with implications for ultramafic-hosted hydrothermal systems at mid-ocean ridges. Geochim. Cosmochim. Acta 71, 3872–3886.

Snow, J.E., Dick, H.J.B., 1995. Pervasive magnesium loss by marine weathering of peridotite. Geochim. Cosmochim. Acta 59, 4219–4235.

Snow, J.E., Reisberg, L., 1995. Os isotopic systematics of the MORB mantle: results from altered abyssal peridotites. Earth Planet. Sci. Lett. 133, 411–421.

Wetzel, L.R., Shock, E.L., 2000. Distinguishing ultramafic-from basalt-hosted submarine hydrothermal systems by comparing calculated vent fluid compositions. J. Geophys. Res. 105 (B4), 8319–8340.

Wolery, T.J., 1992. EQ3/6, a Software Package for Geochemical Modeling of Aqueous Systems: Package Overview and Installation Guide (version 7.0). Lawrence Livermore National Laboratory, Livermore, CA.